Fermi National Accelerator Laboratory

FERMILAB-Conf-96/013-E
CDF

B Physics at CDF

Emilio Meschi
For the CDF Collaboration

Fermi National Accelerator Laboratory
P.O. Box 500, Batavia, Illinois 60510

Universita di Pisa and INFN sez. di Pisa
Via Livornese 582/a - 56100 S. Piero a Grado (PISA) Italy

January 1996

Published Proceedings Conference on *Production and Decay of Hyperons, Charm and Beauty Hadrons*, Strasbourg, France, September 2-8, 1995

Disclaimer

B physics at CDF

Emilio Meschi[a]

[a]Università di Pisa and INFN sez. di Pisa
Via Livornese 582/a - 56100 S.Piero a Grado (PISA) - Italy

Results on B physics and heavy quarkonia production based on data collected during the Tevatron run Ia and Ib are presented. For B physics, results on B meson mass measurement, B meson lifetimes, rare decay searches, $B^0\bar{B}^0$ mixing and B meson polarization are discussed. Accuracies comparable to those of leading e^+e^-experiments are attained or expected to be attained by the end of Tevatron Run I in almost all these fields. Unexpected features of J/ψ , $\psi(2S)$, χ_c, and Υ bound state production are also discussed.

1. INTRODUCTION

At the Fermilab Tevatron, with 1.8 TeV proton-antiproton colliding beams, the b-quark production cross section is quite high. In fact an extrapolation from current cross-section measurements indicates a total cross section of ~ 30 pb^{-1} in the region $|y| < 1$, where most of CDF muon and tracking coverage is. At the luminosities of Run I, of order 10^{31}, this corresponds to about 300 $b\bar{b}$ events per second, or about 30 times the current data logging rate of CDF. On the other side backgrounds are challenging, since the total inelastic cross section is about 1,000 times larger than the total b cross section; most of the $b\bar{b}$ pairs are also produced with very low p_t. This imposes tight requirements on the trigger system, to obtain good acceptance and a reasonably low rate.

CDF has been described in detail elsewhere [1]. Subdetectors that are relevant to the analyses presented here are the four-layer Silicon VerteX detector (SVX) [2], and the Central Tracking Chamber (CTC), which surrounds it; these are immersed in the 1.5 T magnetic field of the CDF superconducting solenoid. Muons are detected by two sets of drift chambers outside the calorimeter, separated by about 50 cm of steel.

CDF b triggers are all based on leptons. Two classes of triggers exist, requiring 1 and 2 leptons, respectively:

1. dilepton triggers: two muons with $p_t > 2$ GeV/c or one muon with $p_t > 2$ GeV/c and one electron with $E_t > 5$ GeV;
2. single lepton triggers: one electron with $E_t > 8$ GeV or one muon with $p_t > 7.5$ GeV/c.

Dilepton triggers are used for J/ψ and ψ', that yield the majority of reconstructed exclusive b decays; away from resonances (including Υ's) they are used for mixing studies and for rare decays search. Single lepton triggers are the source of semi-exclusive b-hadron semileptonic decays and are used for lifetime studies and to measure the production cross-section.

Analyses described in this paper use data from the 1992-95 Collider Run I, most of the results being from Run Ia, in which 20 pb^{-1} were collected, while a few results include data from the first part of Run Ib amounting to ~ 50 pb^{-1}. At the time of writing the total integrated luminosity collected in Run I is 115 pb^{-1}, and CDF is about to resume data-taking for the last part of the run, to collect 30 pb^{-1} more. Expectations by the end of Run I are discussed.

2. B Meson Masses

Taking advantage of the large statistics of the J/ψ and ψ' samples collected, of which ~ 20 % come from $b\bar{b}$ events, CDF has measured the B_u and B_d masses with accuracies that are competitive with e^+e^- experiments, and obtains the best accuracy on the B_s mass measurement.

The analysis starts with the selection of $J/\psi \to \mu^+\mu^-$ events from the dimuon trigger. To select a muon a three dimensional track in the

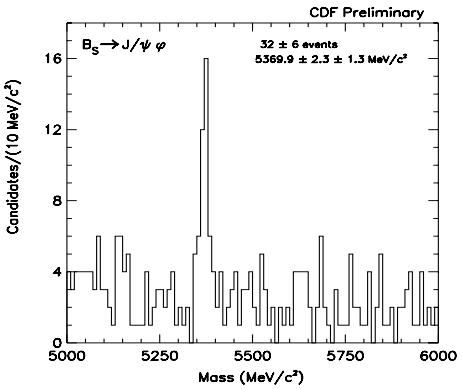

Figure 1. Invariant mass distributions of fully reconstructed B_s candidates.

CTC is required, pointing to a muon track segment in the muon chambers within 3σ, where σ is the uncertainty on the extrapolation taking into account multiple scattering. The invariant mass is then calculated for each opposite sign muon candidate pair, and J/ψ candidates are selected by requiring their invariant mass to be within 100 MeV/c^2 of the world average J/ψ mass. Approximately 80,000 J/ψ 's were found in Run Ia data, with a signal to background ratio of ~ 10.

Specific B meson decay channels are then selected by associating each J/ψ candidate to other charged tracks in the event. B meson masses and decay lengths are obtained by fitting all the tracks to a common secondary vertex, with the constraint that the two muons form the J/ψ invariant mass and that the reconstructed B meson momentum points to the primary vertex.

The decays $B^+ \rightarrow J/\psi K^+$ [1], $B^0 \rightarrow J\psi K^{*0}$, and $B_s^0 \rightarrow J/\psi\phi$, with subsequent decays $K^{*0} \rightarrow K^+\pi^-$ and $\phi \rightarrow K^+K^-$ were used. Requiring $p_t(K^+) > 2$ GeV/c, $p_t(\phi) > 2$ GeV/c, and $p_t(K^*) > 3$ GeV/c, as well as $p_t(B^+) > 8$ GeV/c, $p_t(B^0) > 8$ GeV/c, and $p_t(B_s^0) > 6$ GeV/c, the invariant mass distributions were obtained. As an example in fig.1 we show the invariant mass distribution for the decay $B_s^0 \rightarrow J/\psi\phi$. An additional cut $c\tau(B^+, B^0) > 100\mu$m was also applied, while $c\tau(B_s^0)$ was required to be positive. From

[1] A specific charged status implies the charge conjugate as well, unless otherwise stated

B meson	mass [MeV/c^2]	events
B^+	$5279.1 \pm 1.7 \pm 1.4$	147 ± 14
B^0	$5281.3 \pm 2.2 \pm 1.4$	51 ± 8
B_s	$5369.9 \pm 2.3 \pm 1.3$	32 ± 6

Table 1
Summary of B meson mass measurements; Run Ia (20 pb^{-1}).

a fit to a gaussian peak plus a linear background shape the mass values shown in table 1 were obtained.

The results discussed are based on 20 pb$^-$1 data from Run Ia. By the end of Run I the statistical uncertainties are expected to go down to < 1 MeV/c^2, with a systematic uncertainty[2] also around 1 MeV/c^2.

3. B Meson Lifetimes

Current non-spectator decay models for B mesons predict a small lifetime difference between the charged and neutral B mesons ($\sim 5 - 10$ %). Reaching this precision would also help in understanding the large discrepancy of the observed semileptonic branching fractions with respect to the spectator model [3].

The lifetime measurement requires a very accurate measurement of the primary vertex position. CDF takes advantage of the very small size of the Tevatron luminous region ($\sim 35\mu$m diameter), and of the excellent impact parameter resolution of the SVX.

Two measurements of the $B_{u,d}$ mesons lifetimes are reported here. The first is based on fully reconstructed decays of the type $B \rightarrow \Psi\mathbf{K}$ (all possible channels are used to improve statistics), for which a Midrun update is given, using 70 pb$-$1 of data. The second is a semi-inclusive measurement based on the association of a D^* meson with a lepton. The latter only uses 20 pb^{-1} of data from Run Ia. We also report measurements of the B_s lifetime based on Run Ia data.

[2] Systematic errors are dominated by momentum scale uncertainty (the momentum scale is calibrated using the large sample of J/ψ decays), and tracking systematics.

3.1. Exclusive $B_{u,d}$ Lifetimes

This analysis uses the large sample of 140,000 $J/\psi \to \mu^+\mu^-$ candidates with both muon tracks in the SVX. First a vertex- and mass-constrained fit is applied to the J/ψ candidates, which are then associated with K candidates, where K represents different Kaon states: K^+, $K^*(892)^+$, K_s^0, or $K^*(892)^0$. A vertex-constrained fit of the whole system yields the two dimensional decay length L_{xy}. The $c\tau$ distributions are then obtained using the precision p_t measurement from the CTC (fig.2). The proper time distribution for

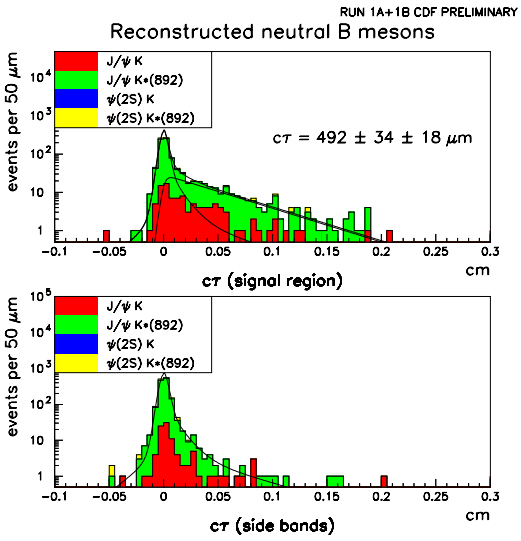

Figure 2. Proper time distributions of neutral B candidates, exemplifying the lifetime fit. The bottom plot represents the background $c\tau$ distribution as obtained from the B sidebands.

the background is obtained by fitting the sidebands of the mass distribution with a gaussian with exponential tails. The $c\tau$ signal distribution is assumed to be an exponential folded with a gaussian resolution. The unbinned likelihood fits give the results shown in table 2.

3.2. Semi-inclusive B lifetimes

The accuracy of the exclusive measurement is still dominated by statistics. To increase statistics one can give up the full reconstruction of the B decay. This semi-inclusive analysis only uses about 20 pb^{-1} of Run Ia single lepton trigger events.

Exclusive lifetime
$\tau(B^+) = 1.68 \pm 0.09 \pm 0.06$ ps
$\tau(B^0) = 1.64 \pm 0.11 \pm 0.06$ ps
$\tau(B^+)/\tau(B^0) = 1.02 \pm 0.09 \pm 0.01$

Table 2
Summary of exclusive B lifetime results.

The analysis principle is as follows: In a cone around the trigger electron or muon, $D^{(*)}$ meson candidates are reconstructed through their decay modes:

1. $D^0 \to K^-\pi^+$, where the D^0 is not from a D^{*+};
2. $D^{*+} \to D^0\pi^+$, $D^0 \to K^-\pi^+$;
3. $D^{*+} \to D^0\pi^+$, $D^0 \to K^-\pi^+X$.
4. $D^{*+} \to D^0\pi^+$, $D^0 \to K^-\pi^+\pi^+\pi^-$;

where 3. is dominated by $D^0 \to K\rho$ and X represents a π^0 which is not reconstructed. A secondary vertex is then defined as the intersection of the D^* and lepton trajectories in the transverse plane, and a transverse decay length obtained. Since the B is not fully reconstructed, its $c\tau$ cannot be directly obtained. A correction has to be applied to scale from the $D^{(*)}\ell$ momentum to $p_t(B)$. This $\beta\gamma$ correction is obtained by means of a Monte Carlo simulation.

The final $D^{(*)}$ candidates can be seen in Fig. 3: (a) $D^0 \to K^-\pi^+$, where the D^0 is not from a D^{*+}, (b) $D^{*+} \to D^0\pi^+$, $D^0 \to K^-\pi^+$, (c) $D^{*+} \to D^0\pi^+$, $D^0 \to K^-\pi^+\pi^+\pi^-$, and (d) $D^{*+} \to D^0\pi^+$, $D^0 \to K^-\pi^+X$. Although the resolution of the D^{*+} mass peak is worse in case (d) compared to the other channels, it is still good enough to use this mode in the analysis. The lifetime distributions obtained from $\ell^+\bar{D}^0$ and ℓ^+D^{*-} are used to determine the individual B^+ and B^0 lifetimes. A $\ell^+\bar{D}^0$ combination usually originates from a charged B while ℓ^+D^{*-}

Exclusive lifetime
$\tau(B^+) = 1.51 \pm 0.12 \pm 0.08$ ps
$\tau(B^0) = 1.57 \pm 0.08 \pm 0.07$ ps
$\tau(B^+)/\tau(B^0) = 0.96 \pm 0.10 \pm 0.05$

Table 3
Summary of semi-inclusive B lifetime results.

comes from a B^0. This simple picture is complicated by the existence of D^{**} states which are the source of $\bar{D}^0$ (D^{*-}) mesons that originate from a decay $B^0 \to D^{**-}\ell^+$, $D^{**-} \to \bar{D}^0 X$ ($B^+ \to \bar{D}^{**0}\ell^+$, $\bar{D}^{**0} \to D^{*-}X$). This cross talk from D^{**} resonances has been decomposed using Monte Carlo. A combined lifetime fit yields the B lifetimes given in Table 3. The main systematic errors arise from the background shape, residual misalignment, the $\beta\gamma$ correction, and the D^{**} sample modeling. We expect the statistical error of this measurement to be reduced by a factor of 2.5 at the end of Run I, while the exclusive lifetimes will only improve by a factor $\sqrt{2}$ since this result already represents a midrun update.

The uncertainty of less than 10% on the CDF exclusive and semi-exclusive B lifetime results compares well to individual lifetime measurements by the LEP experiments [4]

3.3. B_s Lifetime

The lifetime of the B_s meson has been measured on 20 pb^{-1} from Run Ia, using two methods.

The first exploits fully reconstructed decays $B_s \to J/\psi\,\phi$, and a technique analogous to the $B_{u,d}$ case. Using 58 events from $\sim$ 100 pb$^-1$ of integrated luminosity from run Ia + Ib, the lifetime is determined to be $\tau_{B_s} = 1.34^{+0.23}_{-0.19}$(stat.) $\pm$ 0.05(sys.) ps. Although the measurement is statistically limited, this is the single best measurement of the B_s lifetime, and is consistent with other measurements from e^+e^- experiments.

The second method uses partially reconstructed decays in the channel $B_s^0 \to D_s\ell\nu$, $D_s \to \phi\pi$. With 76 events from $\sim$ 20 pb^{-1} (run Ia only), the result is $\tau = 1.42^{+0.27}_{-0.23} \pm 0.11$ ps, where the error is still dominated by statistics.

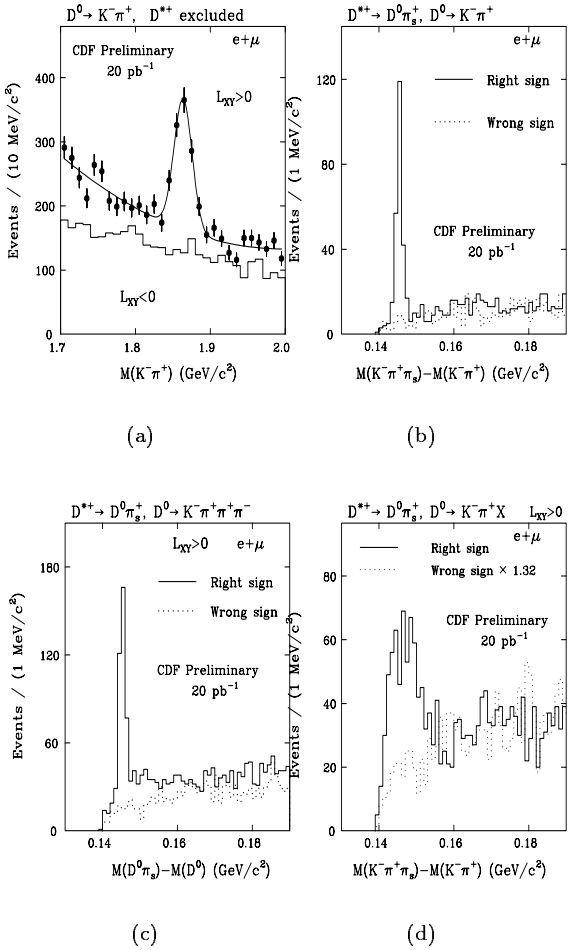

Figure 3. Invariant mass distribution of $D^{(*)}$ candidates from the semi-exclusive lifetime analysis: (a) $D^0 \to K^-\pi^+$, where the D^0 is not from a D^{*+}, (b) $D^{*+} \to D^0\pi^+$, $D^0 \to K^-\pi^+$, (c) $D^{*+} \to D^0\pi^+$, $D^0 \to K^-\pi^+\pi^+\pi^-$, and (d) $D^{*+} \to D^0\pi^+$, $D^0 \to K^-\pi^+X$.

4. Rare B Decays

Because of the large $b\bar{b}$ production cross-section and efficient dimuon triggers CDF is in a favorable position to measure rare B decays with a dimuon in the final state. Limits on the decay $B \to \mu\mu K$ (K is either $K^{\pm}$ or K^{*}), with dimuon invariant mass away from the charmonium resonant region, and on $B \to \mu\mu$ are presented here. These decays are suppressed in the Standard Model. Anomalously large rates would indicate new physics beyond the Standard Model.

For the $\mu\mu K$ search a parallel study is made of the resonant and non-resonant component. In order to minimize the uncertainty on the limit, the non-resonant branching fraction is expressed as a function of the known branching ratio of the decay $B \to J/\psi K$, and the ratio of efficiencies and number of events for each component. The 90% c.l. limits are $\mathrm{BR}(B^{\pm} \to \mu\mu K^{\pm}) < 1.0 \times 10^{-5}$ and $\mathrm{BR}(B^{0} \to \mu\mu K^{*}) < 2.5 \times 10^{-5}$ respectively, to be compared to $\mathrm{BR}(B^{\pm} \to \mu\mu K^{\pm}) < 0.9 \times 10^{-5}$ and $\mathrm{BR}(B^{0} \to \mu\mu K^{*}) < 2.9 \times 10^{-5}$ from CLEO. All of these limits are one to two orders of magnitude larger than the standard model predictions [5], but are expected to improve with the larger statistics available at the end of Run I.

The $B \to \mu\mu$ analysis starts by counting the number of candidate $\mu^{+}\mu^{-}$ pairs with invariant mass in the B_d and B_s mass regions, after $c\tau$ and isolation cuts (see fig. 4). Cut efficiency is estimated mostly from data, and after normalizing to the measured B cross-section for $p_t^B > 6$ GeV/c, the following 90% c.l. limits are obtained:

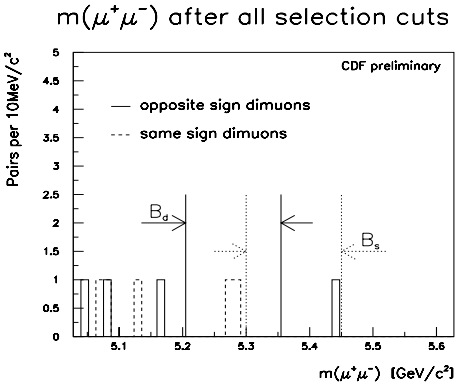

Figure 4.

1. $\mathrm{BR}(B_d \to \mu^{+}\mu^{-}) < 1.6 \times 10^{-6}$, to be compared to a recent CLEO measurement [6]: $\mathrm{BR}(B_d \to \mu^{+}\mu^{-}) < 5.9 \times 10^{-6}$
2. $\mathrm{BR}(B_s \to \mu^{+}\mu^{-}) < 8.4 \times 10^{-6}$

Both results are still several orders of magnitude away from the SM limit.

5. B Polarization

The pseudoscalar to vector-vector decays $B^0 \to J/\psi K^*$ and $B_s^0 \to J/\psi\phi$ allow for two polarization amplitudes to contribute to the final state. The measurement of the net polarization of the final state is a test of the factorization hypothesis for hadronic decays, and can help to determine the contribution of each CP state to the decay, and thus to assess the usefulness of such a decay to study CP violation.

For the first decay a theoretical calculation predicts a longitudinal polarization , $_L$/, ranging from 0.57 to 0.73 [7]. Measurements from ARGUS [8] and CLEO[9] are systematically higher and standard form factor calculations cannot simultaneously explain these values, and the ratio $R =$, $(B \to J/\psi K^*)$/, $(B \to J/\psi K)$ as measured by CLEO [10]

The polarization measurements we describe only use data from CDF Run Ia. The candidate decays were selected with cuts similar to those described in section 2. A few additional cuts were made in order to improve the signal-to-background ratio. The final samples consisted of 65 ± 10 $J/\psi K^*$ events and 19 ± 5 $J/\psi\phi$ events.

An helicity analysis was performed by studying the angular distribution:

$$\frac{d^2,}{d\cos\theta_{K^*}\, d\cos\theta_\psi} \propto \frac{1}{4}\sin^2\theta_{K^*}(1+\cos^2\theta_\psi) \times \times(|H_{+1}|^2 + |H_{-1}|^2) + \cos^2\theta_{K^*}\sin^2\theta_\psi |H_0|^2 \quad (1)$$

where θ_{K^*} is the decay angle of the kaon from the K^* decay in K^* rest frame with respect to the K^* direction in the B rest frame, θ_ψ is the decay angle of the muon in the J/ψ rest frame with respect to J/ψ direction in the B rest frame, and $H_{\pm 1,0}$

are the three helicity amplitudes. Analogous definitions are made for the $J/\psi\phi$ channel.

A two dimensional unbinned likelihood fit of the angular distribution was then performed to obtain the contributions of the two helicity states. The theoretical distribution was weighted by the signal acceptance and a background shape was included as well. The longitudinal polarization is then obtained as

$$\frac{, _L}{,} = \frac{|H_0|^2}{|H_{+1}|^2 + |H_{-1}|^2 + |H_0|^2} \quad (2)$$

The results of the fit are shown in fig. 5, and resulting polarizations summarized in table 4.

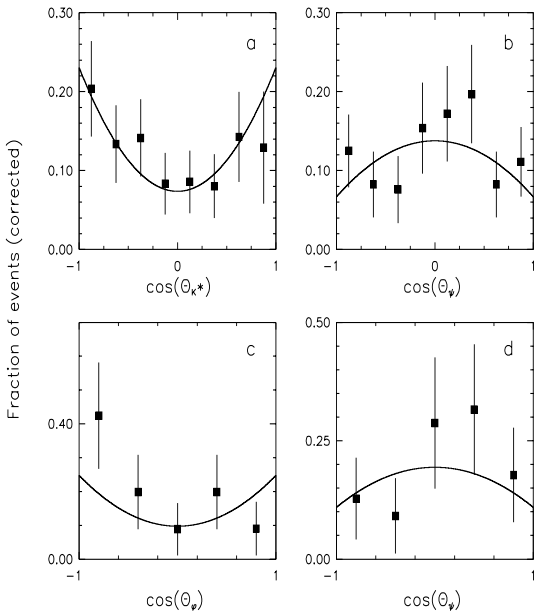

Figure 5. Results of the multidimensional fit to the angular distributions. Dots are data. The fit parameters are the helicity amplitudes.

Combining the CDF result for the B_d polarization with CLEO and ARGUS results, we obtain the world average B_d polarization $, _L/, = 0.74 \pm 0.07$.

Process	$, _L/,$
$B^0 \to J/\psi K^*$	$0.65 \pm 0.10(\text{stat.}) \pm 0.04(\text{sys.})$
(CLEO)	$0.80 \pm 0.08(\text{stat.}) \pm 0.05(\text{sys.})$
(ARGUS)	$0.97 \pm 0.16(\text{stat.}) \pm 0.15(\text{sys.})$
$B_s^0 \to J/\psi\phi$	$0.56 \pm -0.21(\text{stat.})^{+0.02}_{-0.04}(\text{sys.})$

Table 4
Summary of polarization measurements.

6. B Mixing

CDF has measured $B\bar{B}$ mixing using both a time integrated and a time dependent approach. In both cases the flavour of b quarks decaying semileptonically is determined from the sign of the lepton $b \to l^+ + c$ and $\bar{b} \to l^- + \bar{c}$.

6.1. Time-integrated Mixing

In the time-integrated measurement no attempt is made to separate contributions from B_d, B_s and beauty baryons, therefore the mixing parameter measured is $\bar{\chi} = F_d\chi_d + F_s\chi_s$, where the F's are average fractions of B_d and B_s. The ratio, R, of the number of events with like-sign leptons (LS) to the number of opposite-sign (OS) leptons is then related to $\bar{\chi}$ by:

$$R = \left(\frac{LS}{OS}\right) = \left(\frac{2\bar{\chi}(1-\bar{\chi}) + [\bar{\chi}^2 + (1-\bar{\chi})^2]f_s}{\bar{\chi}^2 + (1-\bar{\chi})^2 + 2\bar{\chi}(1-\bar{\chi})f_s + f_c}\right) \quad (3)$$

where f_s is the sequential decay fraction estimated from Montecarlo, and f_c is the charm fraction from $c\bar{c}$ production in the sample, estimated by fitting the p_t^{rel} distribution of the leptons to Montecarlo shapes. The experimental ratio of LS to OS lepton pairs entering (3) must be free of background from fake leptons, this subtraction being a major contribution to the systematic error.

CDF has used the $e\mu$ and $\mu\mu$ channels to measure $\bar{\chi}$. The $e\mu$ channel gives

$$\bar{\chi} = 0.130 \pm 0.010(\text{stat.}) \ \pm 0.009(\text{sys.}).$$

For the $\mu\mu$ channel, we obtain

$$\bar{\chi} = 0.117 \pm 0.020(\text{stat.}) \ \pm 0.026(\text{sys.})$$

For both results the systematic errors are dominated by the uncertainty on the sequential decay fraction.

6.2. Time-dependent Mixing

Low p_t dimuon triggers are used for the time dependent mixing measurement. A secondary vertex tagging algorithm is applied to select events where one of the muons forms a good displaced vertex with at least two other tracks nearby. The tracks used in the vertex fit (excluding the μ) are required to be consistent with a D decay. Substantial backgrounds from sequential decay are rejected by applying a kinematic cut, $p_t^{rel} > 1.3$ of the μ relative to the D^X.

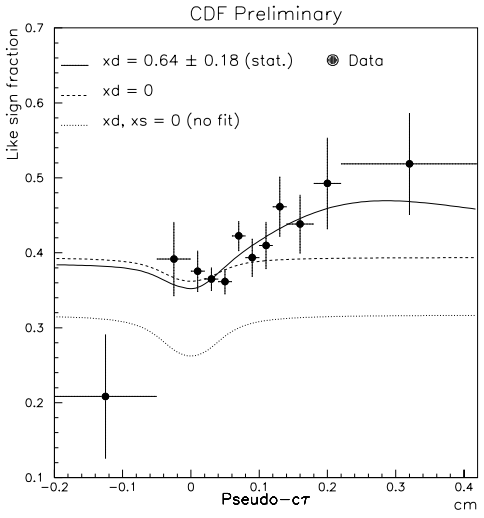

Figure 6. Like-sign fraction versus $c\tau$. The solid line is our fit to the data; the dashed line is our fit after forcing x_d=0 and the dotted line is a prediction assuming just the sequential decay contribution and both x_d and $x_s = 0$

The L_{xy} and proper decay length are obtained in much the same way as the inclusive lifetime analysis. Fig. 6 shows a plot of the like-sign fraction as a function of the pseudo $c\tau$. A clear oscillation signal is observed. To fit the observed oscillation it is necessary to estimate the background, the $c\tau$ resolution function and the sequential decay fraction with its behavior in $c\tau$. The fake fraction is estimated from a fit to the p_t^{rel} distribution. The remaining parameters and resolution functions are obtained from Montecarlo. The final result is:

$$\Delta m_d = 0.44 \pm 0.12 \pm 0.14 \text{ ps}^{-1}$$

The systematic error is dominated by the uncertainty of the sequential fraction. The errors are expected to shrink considerably with larger statistics and a better measurement of f_s from LEP.

7. Quarkonia Production Cross-Sections

CDF has measured the production cross-section for the J/ψ , ψ(2S), χ_c, and Υ.

The $c\bar{c}$ bound states are the first quark bound systems for which perturbative QCD is believed to be applicable. Classic theory describes quarkonium production by the production of a free color singlet $Q\bar{Q}$ state, while the non-perturbative formation of a bound state can be factorized. This scheme predicts the χ_c has by far the largest cross-section and that direct production of J/ψ , ψ(2S) is small. Since the χ_c^0 has a negligible BR to J/ψ , prompt J/ψ were expected to be originated mainly from χ_c^1 and χ_c^2, whereas feed-down is expected to be irrelevant for ψ(2S). The contribution to the overall $c\bar{c}$ production rate from the decay of b flavored hadrons is also important in a collider experiment. At the CDF energy this "non-prompt" (b) component was expected to be dominant for ψ(2S) production, and to contribute significantly to J/ψ production. Prior to the successful operation of the CDF Silicon VerteX (SVX) this picture was not in open disagreement with experiment.

7.1. ψ(2S)

This analysis uses data from Run Ia. The measured production cross-section is $\sigma(|\eta| < 0.6, p_t > 4.0 \text{ GeV/c}) = (94 \pm 8 \pm 9.3 \pm 21 \text{ (BR)})$ nb, where the last uncertainty is that associated with the decay BR. To separate the prompt from the non-prompt component the $c\tau$ distribution is obtained with methods similar to those discussed above; it is then fitted with a long-lived plus a prompt component. The result is that 22.8±3.5% of the ψ(2S) are from b. Since the statistics is high it is possible to perform the fit in various p_t bins

and thus obtain the prompt and non-prompt differential cross-sections. These are shown in fig. 7. Whereas the non-prompt component agrees well with the theory, the prompt cross-section is about a factor of 50 above the theoretical curve. To better understand this anomaly CDF has looked into J/ψ production, to see if this excess is a feature of the ψ(2S) alone.

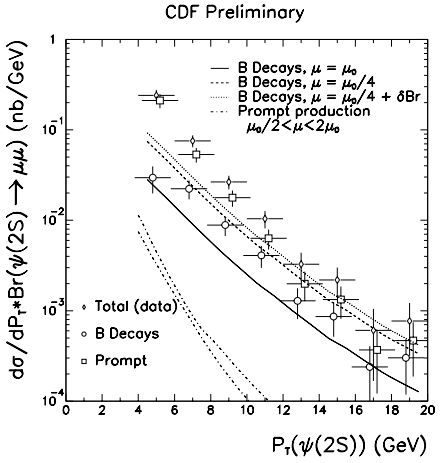

Figure 7. ψ(2S) differential cross-section. The curves are NLO QCD calculations.

7.2. J/ψ

For the J/ψ the measured production cross-section is $\sigma(|\eta| < 0.6,\ P_t > 4.0\ \mathrm{GeV/c}) = (487 \pm 3^{+51}_{-47} \pm 20\ (\mathrm{BR}))$ nb. The prompt and b component are measured from the fit to the pseudo $c\tau$ distribution. The fraction of J/ψ from b is 19.6 ± 1.5 %, similar to the ψ(2S) case, in good agreement with the theory. The prompt component would again be underestimated, but only by a factor of 6. In this case one must distinguish direct J/ψ production, and feed-down from the χ_c system. CDF has measured the fraction of J/ψ from χ_c by reconstructing the decay $\chi_c \rightarrow J/\psi\ \gamma$. A total of 1230 ± 71 such events are observed, the width been too large to distinguish χ_c^1, χ_c^2. After correcting for the photon acceptance and reconstruction efficiency the fraction of J/ψ from χ_c is estimated to be $28 \pm 1.6 \pm 6.8$ %. After having accounted for $B \rightarrow J/\psi$ X and $B \rightarrow \chi_c$ X the fraction of J/ψ from χ_c not from b is $32.3 \pm 2.0(\mathrm{stat.}) \pm 8.5(\mathrm{sys.})$ %. In fig. 8 the various contributions to the cross-sections are shown. The J/ψ from χ_c cross-section is in agreement with the theoretical expectations. The non-χ_c prompt J/ψ cross-section is again a factor of ~ 50 larger than predicted. The color singlet perturbative QCD model of charmonium production fails to describe direct production.

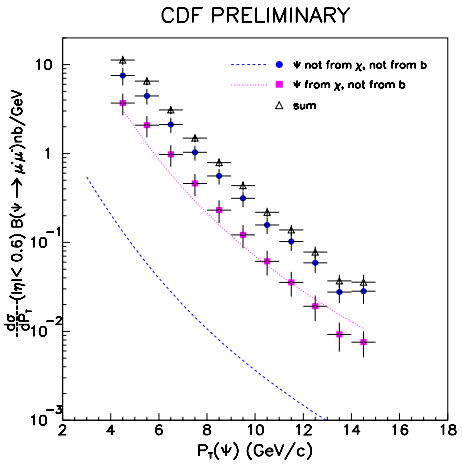

Figure 8. J/ψ differential cross-sections with the contribution from b removed; circles are the direct component, squares the χ_c contribution. The curves are NLO QCD calculations.

CDF has also measured the Υ(1S,2S,3S) production cross-sections. The contribution from χ_b has not yet been separated, and the level of disagreement with theory is around a factor of 3, while the shape is also not reproduced by the theory. Various results from fixed-target experiments show a similar pattern [11].

REFERENCES

1. F. Abe et al. Nucl. Instr. Meth. **A 271**, 387 (1988) and references therein.
2. D. Amidei et al., Nucl. Instr. Meth. **A 350**, 73 (1994). 5 Fermilab, May 9-13,1995.

3. I.I.Bigi, UND-HEP-95-BIG06; to appear in *Proceedings of the 6^{th} International Symposium on Heavy Flavour Physics*, Pisa, Italy, June 6-10,1995.
4. V. Sharma, ibid.
5. A. Ali et al. *Proceedings of the ECFA Workshop on the Physics of the European B Meson Factory*, p.155 (1993).
6. R. Ammar et al. Phys. Rev. D **49**, 5701 (1994).
7. G. Kramer and W.F. Palmer, Phys. Rev. D **46**, 2969 (1992).
8. H. Albrecht et al. Phys. Lett. **B 340**, 217 (1994).
9. M. S. Alam et al. Phys. Rev. **D 50**, 43 (1994).
10. M. Gourdin, A.N. Kamal, and X.Y. Pham, Phys. Rev. Lett. **73**, 3355 (1994).
11. S. Conetti, *This Proceedings.*